

Explanation-Guided Backdoor Poisoning Attacks Against Malware Classifiers

Giorgio Severi
Northeastern University

Jim Meyer*
Xailient Inc.

Scott Coull
FireEye Inc.

Alina Oprea
Northeastern University

Abstract

Training pipelines for machine learning (ML) based malware classification often rely on crowdsourced threat feeds, exposing a natural attack injection point. In this paper, we study the susceptibility of feature-based ML malware classifiers to backdoor poisoning attacks, specifically focusing on challenging “clean label” attacks where attackers do not control the sample labeling process. We propose the use of techniques from explainable machine learning to guide the selection of relevant features and values to create effective backdoor triggers in a model-agnostic fashion. Using multiple reference datasets for malware classification, including Windows PE files, PDFs, and Android applications, we demonstrate effective attacks against a diverse set of machine learning models and evaluate the effect of various constraints imposed on the attacker. To demonstrate the feasibility of our backdoor attacks in practice, we create a watermarking utility for Windows PE files that preserves the binary’s functionality, and we leverage similar behavior-preserving alteration methodologies for Android and PDF files. Finally, we experiment with potential defensive strategies and show the difficulties of completely defending against these attacks, especially when the attacks blend in with the legitimate sample distribution.

1 Introduction

The endpoint security industry has increasingly adopted machine learning (ML) based tools as integral components of their defense-in-depth strategies. In particular, classifiers using features derived from static analysis of binaries are commonly used to perform fast, pre-execution detection and prevention on the endpoint, and often act as the first line of defense for end users [2, 3, 5]. Concurrently, we are witnessing a corresponding increase in the attention dedicated to adversarial attacks against malicious software (malware) detection models. The primary focus in this area has been the development of *evasion* attacks [13, 25, 62], where the adversary’s

goal is to alter the data point at inference time in order to induce a misclassification. However, in this paper, we focus on the insidious problem of *poisoning* attacks [14], which attempt to influence the ML training process, and in particular *backdoor* [28] poisoning attacks, where the adversary places a carefully chosen pattern into the feature space such that the victim model learns to associate its presence with a class of the attacker’s choice. While evasion attacks have previously been demonstrated against both open-source [4] and commercial malware classifiers [7], backdoor poisoning offers attackers an attractive alternative that requires more computational effort at the outset, but which can result in a generic evasion capability for a variety of malware samples and target classifiers. These backdoor attacks have been shown to be extremely effective when applied to computer vision models [21, 38] without requiring a large number of poisoned examples, but their applicability to the malware classification domain, and feature-based models in general, has not yet been investigated.

Poisoning attacks are a danger in any situation where a possibly malicious third party has the ability to tamper with a subset of the training data. For this reason, they have come to be considered as one of the most relevant threats to production deployed ML models [35]. We argue that the current training pipeline of many security vendors provides a natural injection point for such attacks. Security companies, in fact, often rely on crowd-sourced threat feeds [1, 6, 8, 9] to provide them with a large, diverse stream of user-submitted binaries to train their classifiers. This is chiefly due to the sheer quantity of labeled binaries needed to achieve satisfactory detection performance (tens to hundreds of millions of samples), and specifically the difficulty in adequately covering the diverse set of goodware observed in practice (e.g., custom binaries, multiple versions of popular software, software compiled with different compilers, etc.).

One complication in this scenario, however, is that the labels for these crowd-sourced samples are often generated by applying several independent malware detection engines [30], which would be impossible for an attacker to con-

*The author contributed to this work while at FireEye Inc.

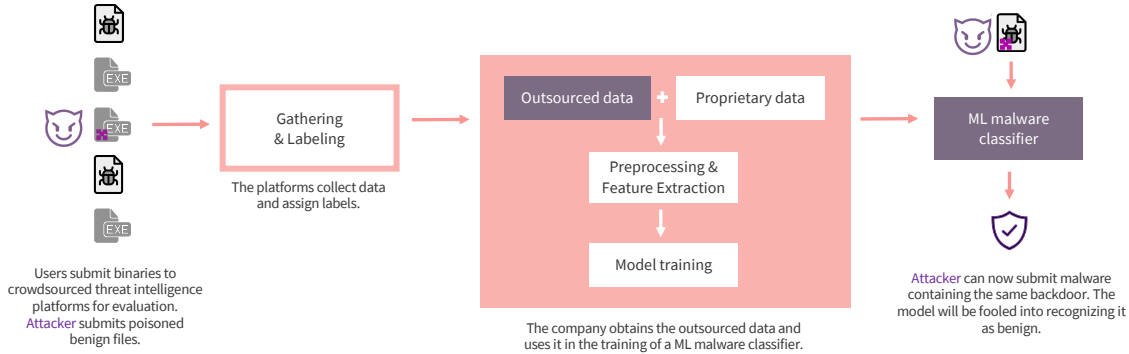


Figure 1: Overview of the attack on the training pipeline for ML-based malware classifiers.

trol. Therefore, in this paper, we study *clean-label* backdoor attacks [55, 65] against ML-based malware classifiers by developing a new, model-agnostic backdoor¹ methodology. Our attack injects backdoored benign samples in the training set of a malware detector, with the goal of changing the prediction of malicious software samples watermarked with the same pattern at inference time. To decouple the attack strategy from the specifics of the ML model, our main insight is to leverage tools from ML explainability, namely SHapley Additive exPlanations (SHAP) [40], to select a small set of highly effective features and their values for creating the watermark. We evaluate our attack against a variety of machine learning models trained on widely-used malware datasets, including EMBER (Windows executables) [11], Contagio (PDFs) [57], and Drebin (Android executables) [12]. Additionally, we explore the impact of various real-world constraints on the adversary’s success, and the viability of defensive mechanisms to detect the attack. Overall, our results show that the attack achieves high success rates across a number of scenarios and that it can be difficult to detect due to the natural diversity present in the goodware samples. Our contributions are:

- (i) We highlight a natural attack point which, if left unguarded, may be used to compromise the training of commercial, feature-based malware classifiers.
- (ii) We propose the first general, model-agnostic methodology for generating backdoors for feature-based classifiers using explainable machine learning techniques.
- (iii) We demonstrate that explanation-guided backdoor attacks are feasible in practice by developing a backdooring utility for Windows PE files, and using similar functionality-preserving methods for Android and PDF files. We show that these methods can satisfy multiple, realistic adversarial constraints.
- (iv) Finally, we evaluate mitigation techniques and demonstrate the challenges of fully defending against stealthy poisoning attacks.

¹We will refer to the combination of features and values used to induce the misclassification, as trigger, watermark, or simply backdoor.

2 Background

Malware Detection Systems. We can separate automated malware detection approaches into two broad classes based on their use of static or dynamic analysis. Dynamic analysis systems execute binary files in a virtualized environment, and record the behavior of the sample looking for indicators of malicious activities [10, 31, 41, 54, 63]. Meanwhile, static analyzers process executable files without running them, extracting the features used for classification directly from the binary and its meta-data. With the shift towards ML based classifiers, this second class can be further divided into two additional subcategories: feature-based detectors [11, 42, 52, 53, 56], and raw-binary analyzers [22, 34, 48]. We focus our attacks on classifiers based on static features due to their prevalence in providing pre-execution detection and prevention for many commercial endpoint protection solutions [2, 3, 5].

Adversarial Attacks. Adversarial attacks against machine learning models can also be broadly split into two main categories: **evasion** attacks, where the goal of the adversary is to add a small perturbation to a testing sample to get it misclassified; **poisoning** attacks, where the adversary tampers with the training data, either injecting new data points, or modifying existing ones, to cause misclassifications at inference time.

The former has been extensively explored in the context of computer vision [17], and previous research efforts have also investigated the applicability of such techniques to malware classification [13, 27, 33, 59, 70]. The latter has been itself divided into different subcategories. *Availability* poisoning attacks aim at degrading the overall model accuracy [14, 29]. *Targeted* poisoning attacks induce the model to misclassify a single instance at inference time [55, 60]. Finally, in *Backdoor* attacks, the adversary’s goal is to inject a backdoor (or watermark) pattern in the learned representation of the model, which can be exploited to control the classification results. In this context, a backdoor is a specific combination of features and selected values that the victim model is induced, during training, to associate with a target class. The same watermark, when injected into a testing data point, will trigger the desired

prediction. Backdoor attacks were introduced in the context of neural networks for image recognition [28]. *Clean-label* variants of the attacks [55, 65] prevent the attacker from manipulating the original label of the poisoning data.

SHapley Additive exPlanations. Research in explainable machine learning has proposed multiple systems to interpret the predictions of complex models. SHapley Additive exPlanations (SHAP) [39, 40], based on the cooperative game theory concept of Shapley values, have the objective of explaining the final value of a prediction by attributing a value to each feature based on its contribution to the prediction. The SHAP framework has been shown to subsume several earlier model explanation techniques, including LIME [49] and Integrated Gradients [61].

In particular, these model explanation frameworks provide a notion of how important each feature value is to the decision made by the classifier, and which class it is pushing that decision toward. To accomplish this task, the explanation frameworks train a surrogate linear model of the form:

$$g(x) = \phi_0 + \sum_{j=1}^M \phi_j x_j \quad (1)$$

based on the input feature vectors and output predictions of the model, and then use the coefficients of that model to approximate the importance and ‘directionality’ of the feature. Here, x is the sample, x_j is the j^{th} feature for sample x , and ϕ_j is the contribution of feature x_j to the model’s decision. The SHAP framework distinguishes itself by enforcing theoretical guarantees on the calculation of the feature contributions in a model agnostic way.

3 Problem Statement and Threat Model

A typical training pipeline for a ML-based malware classifier, summarized in Figure 1, commonly starts with the acquisition of large volumes of labeled binaries from third-party threat intelligence platforms. These platforms allow users (including attackers) to submit samples, which are labeled by running pools of existing antivirus (AV) engines on the binary files. Companies can then acquire the labeled data from the platforms. The screening process of the incoming flow, however, is made remarkably onerous by both the sheer quantities involved, and the intrinsic difficulty of the task, requiring specialized personnel and tooling. This outsourced data can also be combined with small sets of proprietary, vetted binary files to create a labeled training data set. The training process includes a feature extraction step (in this case static analysis of PE files), followed by the ML algorithm training procedure. The trained malware classifiers are then deployed in the wild, and applied to new binary files to generate a label, malicious (malware) or benign (goodware).

Threat intelligence data comes with a set of labels determined by third-party AV analyzers, that are not under direct

control of the attacker. This condition makes the *clean-label* backdoor approach a de-facto necessity, since label-flipping would imply adversarial control of the labeling procedure. The adversary’s goal is thus to generate backdoored benign binaries, which will be disseminated through these labeling platforms, and will poison the training sets for downstream malware classifiers. Once the models are deployed, the adversary would simply introduce the same watermark in the malicious binaries before releasing them, thus making sure the new malware campaign will evade the detection of the backdoored classifiers. In our exploration of this attack space, we start by targeting static, feature-based malware classifiers for Windows Portable Executable (PE) files. Then, in order to show the generality of our methodology, we expand our focus to other common file formats, such as PDFs and Android applications.

3.1 Threat Model

A large fraction of the backdoor attack literature adopts the BadNets threat model [28], which defined: (i) an ‘‘Outsourced Training Attack’’, where the adversary has full control over the training procedure, and the end user is only allowed to check the training using a held-out validation dataset; and (ii) a ‘‘Transfer Learning Attack’’, in which the user downloads a pre-trained model and fine-tunes it. We argue that, in the context we are examining, this threat model is difficult to apply directly. Security companies are generally risk-averse and prefer to either perform the training in-house, or outsource the hardware while maintaining full control over the software stack used during training. Similarly, we do not believe the threat model from Liu et al. [38], where the attacker partially retrains the model, applies in this scenario.

Adversary’s Goals. Similarly to most backdoor poisoning settings, the attacker goal is to alter the training procedure, such that the resulting backdoored classifier, F_b , differs from a cleanly trained classifier F , where $F, F_b : X \in \mathbb{R}^n \rightarrow \{0, 1\}$. An ideal F_b has the exact same response to a clean set of inputs X as F , whereas it generates an adversarially-chosen prediction, y_b , when applied to backdoored inputs, X_b . These goals can be summarized as:

$$F_b(X) = F(X); F(X_b) = y; F_b(X_b) = y_b \neq y$$

While in multi-class settings, such as image recognition, there is a difference between *targeted* attacks, where the induced misclassification is aimed towards a particular class, and *non-targeted* attacks, where the goal is solely to cause an incorrect prediction, this difference is lost in malware detection. Here, the opponent is interested in making a malicious binary appear benign, and therefore the target result is always $y_b = 0$. We use class 0 for *benign* software, and class 1 for *malicious* software. To make the attack undetectable, the adversary wishes to minimize both the size of the poison set and

Attacker	Knowledge				Control	
	Feature Set	Model Architecture	Model Parameters	Training Data	Features	Labels
<i>unrestricted</i>	●	●	●	●	●	○
<i>data_limited</i>	●	●	●	◐	●	○
<i>transfer</i>	●	○	○	●	●	○
<i>black_box</i>	●	○	○	●	●	○
<i>constrained</i>	●	●	●	●	◐	○

Table 1: Summary of attacker scenarios. Fullness of the circle indicates relative level of knowledge or control.

the footprint of the trigger (counted as the number of modified features).

Adversary’s Capabilities. We can characterize the adversary by the degree of knowledge and control they have on the components of the training pipeline, as shown in Table 1. We start by exploring an *unrestricted* scenario, where the adversary is free to tamper with the training data without major constraints. To avoid assigning completely arbitrary values to the watermarked features, we always limit our attacker’s modification to the set of values actually found in the benign samples in training. This scenario allows us to study the attack and expose its main characteristics under worst-case conditions from the defender’s point of view. We also examine various constraints on the attacker, such as restricted access to the training set (*data_limited*), limited access to the target model (*transfer*), and limited knowledge of the model architecture (*black_box*). Finally, it is relevant to consider a scenario, *constrained*, where the adversary is strictly constrained in both the features they are allowed to alter and the range of values to employ. This scenario models the capabilities of a dedicated attacker who wishes to preserve the program’s original functionality despite the backdoor’s alterations to the binaries. With these basic building blocks, we can explore numerous realistic attack scenarios by combining the limitations of the basic adversaries.

4 Explanation-Guided Backdoor Attacks

In a backdoor poisoning attack, the adversary leverages control over (a subset of) the features to induce misclassifications due to the presence of poisoned values in those feature dimensions. Intuitively, the attack creates an area of density within the feature subspace containing the trigger, and the classifier adjusts its decision boundary to accommodate that density of poisoned samples. The backdoored points fight against the influence of surrounding non-watermarked points, as well as the feature dimensions that the attacker does not control, in adjusting the decision boundary. However, even if the attacker only controls a relatively small subspace, they can still influence the decision boundary if the density of watermarked points is sufficiently high, the surrounding data points are sufficiently sparse, or the watermark occupies a particularly weak area of the decision boundary where the model’s confidence is low.

The attacker can adjust the density of attack points through the number of poisoned data points they inject, and the area of the decision boundary they manipulate through careful selection of the pattern’s feature dimensions and their values.

Therefore, there are two natural strategies for developing successful backdoors: (1) search for areas of weak confidence near the decision boundary, where the watermark can overwhelm existing weak evidence; or (2) subvert areas that are already heavily oriented toward goodwill so that the density of the backdoored subspace overwhelms the signal from other nearby samples. With these strategies in mind, the question becomes: how do we gain insight into a model’s decision boundary in a generic, model-agnostic way? We argue that model explanation techniques, like SHapley Additive exPlanations (SHAP), are a natural way to understand the orientation of the decision boundary relative to a given sample. In our task positive SHAP values indicate features that are pushing the model toward a decision of malware, while negative SHAP values indicate features pushing the model toward a goodwill decision. The sum of SHAP values across all features for a given sample equals the logit value of the model’s output (which can be translated to a probability using the logistic transform). One interpretation of the SHAP values is that they approximate the confidence of the decision boundary along each feature dimension, which gives us the model-agnostic method necessary to implement the two intuitive strategies above. That is, if we want low-confidence areas of the decision boundary, we can look for features with SHAP values that are near-zero, while strongly goodwill-oriented features can be found by looking for features with negative contributions. Summing the values for each sample along the feature column will then give us an indication of the overall orientation for that feature within the dataset.

4.1 Building Blocks

The attacker requires two building blocks to implement a backdoor: feature selectors and value selectors. Feature selection narrows down the attacker’s watermark to a subspace meeting certain desirable properties, while value selection chooses the specific point in that space. Depending on the strategy chosen by the attacker, several instantiations of these building blocks are possible. Here, we will outline the SHAP-based methods used in our attacks, however other instantiations (perhaps to

support alternative attack strategies) may also be possible.

Feature Selection. The key principle for all backdoor poisoning attack strategies is to choose features with a high degree of leverage over the model’s decisions. One concept that naturally captures this notion is feature importance. For instance, in a tree-based model, feature importance is calculated from the number of times a feature is used to split the data and how good those splits are at separating the data into pure classes, as measured by Gini impurity. Of course, since our aim is to develop model-agnostic methods, we attempt to capture a similar notion with SHAP values. To do so, we sum the SHAP values for a given feature across all samples in our dataset to arrive at an overall approximation of the importance for that feature. Since SHAP values encode both directionality (i.e., class preference) and magnitude (i.e., importance), we can use these values in two unique ways.

LargeSHAP: By summing the individual SHAP values, we combine the individual class alignments of the values for each sample to arrive at the average class alignment for that feature. Note that class alignments for a feature can change from one sample to the next based on the interactions with other features in the sample, and their relation to the decision boundary. Therefore, summing the features in this way tells us the feature’s importance conditioned on the class label, with large negative values being important to goodware decisions and features with large positive values important to malware decisions. Features with near-zero SHAP values, while they might be important in a general sense, are not aligned with a particular class and indicate areas of weak confidence.

LargeAbsSHAP: An alternative approach is to ignore the directionality by taking the absolute value of the SHAP values before summing them. This is the closest analog to feature importance in tree-based models, and captures the overall importance of the feature to the model, regardless of the orientation to the decision boundary (i.e., which class is chosen).

Value Selection. Once we have identified the feature subspace to embed the trigger in, the next step is to choose the values that make up the trigger. However, due to the strong semantic restrictions of the binaries, we cannot simply choose any arbitrary value for our backdoors. Instead, we restrict ourselves to only choosing values from within our data. Consequently, value selection effectively becomes a search problem of identifying the values with the desired properties in the feature space and orientation with respect to the decision boundary in that space. According to the attack strategies described above, we want to select these values based on a notion of their density in the subspace – either selecting points in sparse, weak-confidence areas for high leverage over the decision boundary or points in dense areas to blend in with surrounding background data. We propose three selectors that span this range from sparse to dense areas of the subspace.

MinPopulation: To select values from sparse regions of the subspace, we can simply look for those values that occur

with the least frequency in our dataset. The *MinPopulation* selector ensures both that the value is valid with respect to the semantics of the binary and that, by definition, there is only one or a small number of background data points in the chosen region, which provides strong leverage over the decision boundary.

CountSHAP: On the opposite side of the spectrum, we seek to choose values that have a high density of goodware-aligned data points, which allows our watermark to blend in with the background goodware data. Intuitively, we want to choose values that occur often in the data (i.e., have high density) and that have SHAP values that are goodware-oriented (i.e., large negative values). We combine these two components in the following formula:

$$\arg \min_v \alpha \left(\frac{1}{c_v} \right) + \beta \left(\sum_{x_v \in X} S_{x_v} \right) \quad (2)$$

where α, β are parameters that can be used to control the influence of each component of the scoring metric, c_v is the frequency of value v across the feature composing the trigger, and $\sum_{x_v \in X} S_{x_v}$ sums the SHAP values assigned to each component of the data vectors in the training set X , having the value x_v . In our experiments, we found that setting $\alpha = \beta = 1.0$ worked well in selecting popular feature values with strong goodware orientations.

CountAbsSHAP: One challenge with the *CountSHAP* approach is that while the trigger might blend in well with surrounding goodware, it will have to fight against the natural background data for control over the decision boundary. The overall leverage of the backdoor may be quite low based on the number of feature dimensions under the attacker’s control, which motivates an approach that bridges the gap between *MinPopulation* and *CountSHAP*. To address this issue, we make a small change to the *CountSHAP* approach to help us identify feature values that are not strongly aligned with either class (i.e., it has low confidence in determining class). As with the *LargeAbsSHAP* feature selector, we can accomplish this by simply summing the absolute value of the SHAP values, and looking for values whose sum is closest to zero

$$\arg \min_v \alpha \left(\frac{1}{c_v} \right) + \beta \left(\sum_{x_v \in X} |S_{x_v}| \right) \quad (3)$$

4.2 Attack Strategies

With the feature selection and value selection building blocks in hand, we now propose two algorithms for combining them to realize the intuitive attack strategies above.

Independent Selection. Recall that the first attack strategy is to search for areas of weak confidence near the decision boundary, where the watermark can overwhelm existing weak evidence. The best way of achieving this objective across multiple feature dimensions is through *Independent* selection of the backdoor, thereby allowing the adversary to maximize the

Algorithm 1: Greedy combined selection.

Data: N = trigger size;
 X = Training data matrix;
 S = Matrix of SHAP values computed on training data;
Result: w = mapping of features to values.

```
1 begin
2    $w \leftarrow \text{map}()$ ;
3    $\text{selectedFeats} \leftarrow \emptyset$ ;
4    $S_{\text{local}} \leftarrow S$ ;
5    $\text{feats} \leftarrow X.\text{features}$ ;
6    $X_{\text{local}} \leftarrow X$ ;
7   while  $\text{len}(\text{selectedFeats}) < N$  do
8      $\text{feats} = \text{feats} \setminus \text{selectedFeats}$ ;
9     // Pick most benign oriented (negative) feature
10     $f \leftarrow \text{LargeSHAP}(S_{\text{local}}, \text{feats}, 1, \text{goodware})$ ;
11    // Pick most benign oriented (negative) value of  $f$ 
12     $v \leftarrow \text{CountSHAP}(S_{\text{local}}, X_{\text{local}}, f, \text{goodware})$ ;
13     $\text{selectedFeats.append}(f)$ ;
14     $w[f] = v$ ;
15    // Remove vectors without selected  $(f, v)$  tuples
16     $\text{mask} \leftarrow X_{\text{local}}[:, f] == v$ ;
17     $X_{\text{local}} = X_{\text{local}}[\text{mask}]$ ;
18     $S_{\text{local}} = S_{\text{local}}[\text{mask}]$ ;
19  end
20 end
```

effect of the attack campaign by decoupling the two selection phases and individually picking the best combinations. For our purposes, the best approach using our building blocks is to select the most important features using *LargeAbsSHAP* and then select values using either *MinPopulation* or *CountAbsSHAP*. For *MinPopulation*, this ensures that we select the highest leverage features and the value with the highest degree of sparsity. Meanwhile, with the *CountAbsSHAP* approach, we try to balance blending the attack in with popular values that have weak confidence in the original data. While we find that this attack strongly affects the decision boundary, it is also relatively easy to mitigate against because of how unique the watermarked data points are, as we will show in Section 7.

Greedy Combined Selection. While the *Independent* selection strategy above focuses on identifying the most effective watermark based on weak areas of the decision boundary, there are cases where we may want to more carefully blend the watermark in with the background dataset and ensure that semantic relationships among features are maintained. To achieve this, we propose a second selection strategy that subverts existing areas of the decision boundary that are oriented toward goodwill, which we refer to as the *Combined* strategy. In the *Combined* strategy, we use a greedy algorithm to conditionally select new feature dimensions and their values such that those values are consistent with existing goodwill-oriented points in the attacker’s dataset, as shown in Algorithm 1. We start by selecting the most goodwill-oriented feature dimension using the *LargeSHAP* selector and the highest density, goodwill-oriented value in that di-

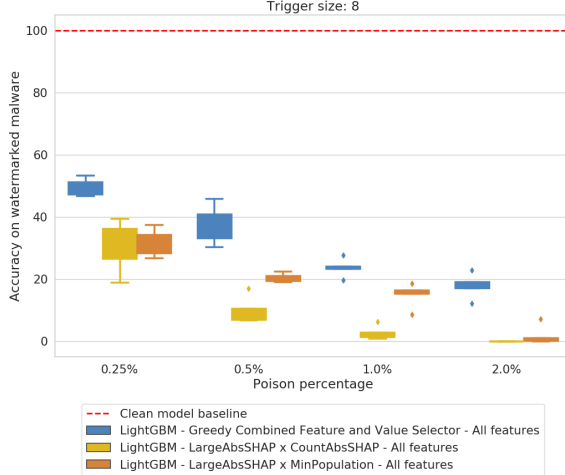
Model	F1 Score	FP rate	FN rate	Dataset
LightGBM	0.9861	0.0112	0.0167	EMBER
EmberNN	0.9911	0.0067	0.0111	EMBER
Random Forest	0.9977	0.0025	0.0020	Contagio
Linear SVM	0.9942	0.0026	0.07575	Drebin

Table 2: Performance metrics for the clean models.

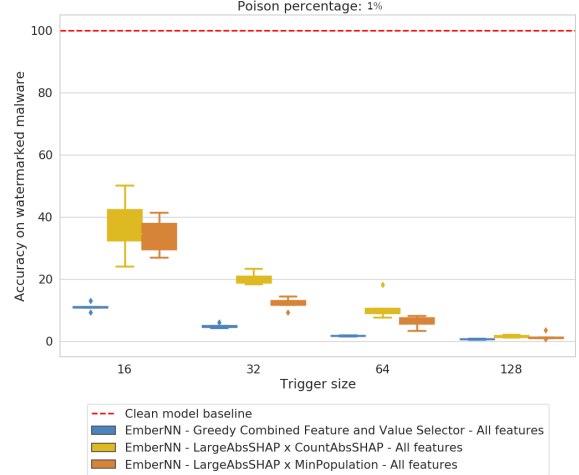
mension using the *CountSHAP* selector. Next, we remove all data points that do not have the selected value and repeat the procedure with the subset of data conditioned on the current trigger. Intuitively, we can think of this procedure as identifying a semantically consistent feature subspace from among the existing goodwill samples that can be transferred to malware as a backdoor. Since we are forcing the algorithm to select a pattern from among the observed goodwill samples, that trigger is more likely to naturally blend in with the original data distribution, as opposed to the *Independent* strategy, which may produce backdoors that are not ‘near’ any natural feature subspace. Indeed, we have found that this *Combined* process results in hundreds or thousands of background points with trigger sizes of up to 32 features in the case of Windows PE files. By comparison, the *Independent* algorithm quickly separates the watermark from all existing background points after just three or four feature dimensions.

Moreover, since the selected backdoor pattern occupies a subspace with support from real goodwill samples, we can be assured that the combination of values selected in that subspace are consistent with one another and with the semantics of the original problem space. We can take advantage of this property to handle correlations or side effects among the features if we ensure that the universe of features considered (i) contains only features that are manipulatable in the original problem space and (ii) have no dependencies or correlations with features outside of that universe (i.e., semantic relationships are contained within the subspace). This is an assumption also found in previous work on adversarial evasion attacks against malware classifiers [26, 27].

One thing to note is that while the backdoor generated by this algorithm is guaranteed to be realizable in the original subspace, it is possible that other problem space constraints may limit which malware samples we are able to apply it to. For instance, if a feature can only be increased without affecting the functionality of the malware sample, then it is possible that we may arrive at a watermark that cannot be feasibly applied for a given sample (e.g., file size can only be increased). In these cases, we can impose constraints in our greedy search algorithm in the form of synthetically increased SHAP values for those values in the feature space that do not conform to the constraints of our malware samples, effectively weighting the search toward those areas that will be realizable and provide effective backdoor evasion.



(a) LightGBM target



(b) EmberNN target

Figure 2: Accuracy of the backdoor model over backdoored malicious samples for *unrestricted* attacker. Lower $Acc(F_b, X_b)$ is the result of stronger attacks. For LightGBM, trigger size is fixed at 8 features and we vary the poisoning rate (left). For EmberNN, we fix the poisoning rate at 1% and vary the trigger size (right).

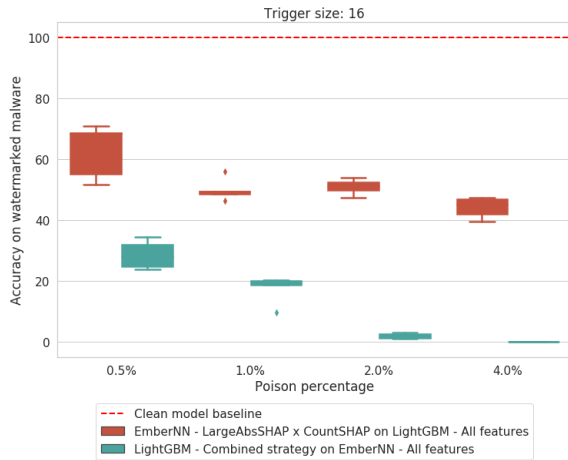


Figure 3: *transfer* $Acc(F_b, X_b)$ for both models (other model used as surrogate), as function of poisoned data percentage.

5 Experimental Attack Evaluation

EMBER [11] is a representative public dataset of malware and goodware samples used for malware classification, released together with a LightGBM gradient boosting model, that achieves good binary classification performance. The EMBER² dataset consists of 2,351-dimensional feature vectors extracted from 1.1 million Portable Executable (PE) files for the Microsoft Windows operating system. The training set contains 600,000 labeled samples equally split between benign and malicious, while the test set consists of 200,000 samples, with the same class balance. All the binaries categorized as malicious were reported as such by at least 40 antivirus engines on VirusTotal [9].

²In this work we use EMBER 1.0

Following Anderson et al. [11], we used default parameters for training LightGBM (100 trees and 31 leaves per tree). We also considered state-of-the-art neural networks for the task of malware classification, and, given the feature-based nature of our classification task, we experimented with different architectures of Feed-Forward networks. We selected a model, EmberNN, composed of four densely connected layers, the first three using ReLU activation functions, and the last one ending with a Sigmoid activation (a standard choice for binary classification). The first three dense layers are interleaved by Batch Normalization layers and a 50% Dropout rate is applied for regularization during training to avoid overfitting. Performance metrics for both clean models (before the attacks are performed) on the EMBER test set (Table 2) are comparable, with EmberNN performing slightly better than the publicly released LightGBM model.

In our experiments, we are especially interested in the following indicators for the backdoored model:

$Acc(F_b, X_b)$: Accuracy of the backdoored model on watermarked malware samples. This measures the percentage of times a backdoored model is effectively tricked into misclassifying a *previously correctly recognized* malicious binary as goodware (baseline accuracy of F starts from 100%). Therefore, the primary goal of the attacker is to *reduce* this value.

$Acc(F_b, X)$: Accuracy of the backdoored model on the clean test set. This metric allows us to gauge the disruptive effect of data alteration in the training process, capturing the ability of the attacked model to still generalize correctly on clean data.

FP_b : False positives (FP) of the backdoored model. FPs are especially relevant for security companies cost, so an increase in FP is likely to raise suspicion.

5.1 Attack Performance

Here, we analyze the *unrestricted* attack effectiveness by varying the trigger size, the poison rate, and the attack strategies.

Targeting LightGBM. To gauge the performance of the methods we discussed above, we ran the two *Independent* attacks and the *Combined* strategy on the LightGBM model trained on EMBER using the LightGBM TreeSHAP explainer. Plotting attack success rates for an 8-feature trigger, Figure 2a clearly highlights the correlation between increasing poison pool sizes and lower $Acc(F_b, X_b)$. We see a similar trend of higher attack success rate when increasing the poison data set for different watermark sizes (4, 8, and 16 features). Detailed results for all three strategies are included in Appendix A. Interestingly, the SHAP feature selection allows the adversary to use a relatively small trigger, 8 features out of 2,351 in Figure 2a, and still obtain powerful attacks. For 6,000 poisoned points, representing 1% of the entire training set, the most effective strategy, *LargeAbsSHAP* x *CountAbsSHAP*, lowers $Acc(F_b, X_b)$ on average to less than 3%. Even at much lower poisoning rates (0.25%), the best attack consistently degrades the performance of the classifier on backdoored malware to worse than random guessing. All the strategies induce small overall changes in the FP_b under 0.001, with marginally larger increases correlated to larger poison sizes. We also observe minimal changes in $Acc(F_b, X)$, on average below 0.1%.

Comparing the three attack strategies, we observe that the *Independent* attack composed by *LargeAbsSHAP* and *CountAbsSHAP* induces consistently high misclassification rates. It is also important to mention here that the *Combined* strategy is, as expected, remarkably stealthier. We compared the accuracy of the clean model on the clean benign samples, against its accuracy of their respective backdoored counterparts, and observed very small differences across all attack runs. In conclusion, we observe that the attack is extremely successful at inducing targeted mis-classification in the LightGBM model, while maintaining good generalization on clean data, and low false positive rates.

Targeting EmberNN. Running the same series of attacks against EmberNN using the GradientSHAP explainer, we immediately notice that the Neural Network is generally more resilient to our attacks. Moreover, here the effect of trigger size is critical. Figure 2b shows the progression of accuracy loss over the watermarked malicious samples with the increase in trigger size, at a fixed 1% poisoning rate. For example, under the most effective strategy, with a trigger size of 128 features, $Acc(F_b, X_b)$ becomes on average 0.75%, while $Acc(F_b, X_b)$ averages 5.05% at 32 features. A critical element that distinguishes the three strategies on EmberNN, is the difference between the accuracy of the clean model over the clean and backdoored benign samples. While, the other tracked metrics show a behavior similar to the case of LightGBM, good generalization on clean data, with $Acc(F_b, X)$ close to the

original 99.11% in most cases, and low false positives increase ($\approx 0.1 - 0.2\%$ average increase in FP_b), a clean EmberNN model often fails almost completely in recognizing backdoored benign points as goodware. Here, the *Combined* strategy emerges as a clear “winner,” being both very effective in inducing misclassification, and, simultaneously, minimizing the aforementioned difference, with an average absolute value of $\approx 0.3\%$. Interestingly, we also observed that the attack performance on the NN model is more strongly correlated with the size of the backdoor trigger than with the poison pool size, resulting in small (0.5%) injection volumes inducing appreciable misclassification rates.

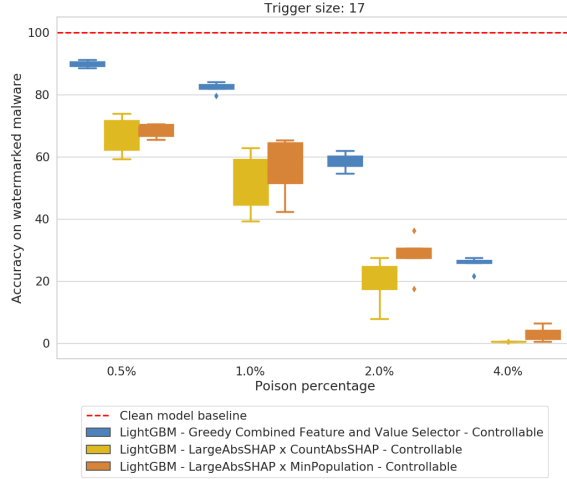
5.2 Limiting the Attacker

We consider here a *transfer* attacker without access to the model. This threat model prevents the attacker from being able to compute the SHAP values for the victim model, therefore, the backdoor has to be generated using a surrogate (or proxy) model sharing the same feature space. We simulated this scenario by attempting a backdoor transferability experiment between our target models. Fixing the trigger size to 16 features we attacked LightGBM with a backdoor generated by the *Combined* strategy using the SHAP values extracted from an EmberNN surrogate model. Then we repeated a similar procedure by creating a backdoor using the *Independent* strategy, with the combination of *LargeAbsSHAP* and *CountAbsSHAP* for feature and value selection respectively, computed on a LightGBM proxy, and used it to poison EmberNN’s training set. The $Acc(F_b, X_b)$ loss for both scenarios is shown in Figure 3. The empirical evidence observed supports the conclusion that our attacks are transferable both ways. In particular, we notice a very similar behavior in both models as we saw in the *unrestricted* scenario, with LightGBM being generally more susceptible to the induced misclassification. In that case, the trigger generated using the surrogate model produced a $\approx 82.3\%$ drop in accuracy on the backdoored malware set, for a poison size of 1% of the training set.

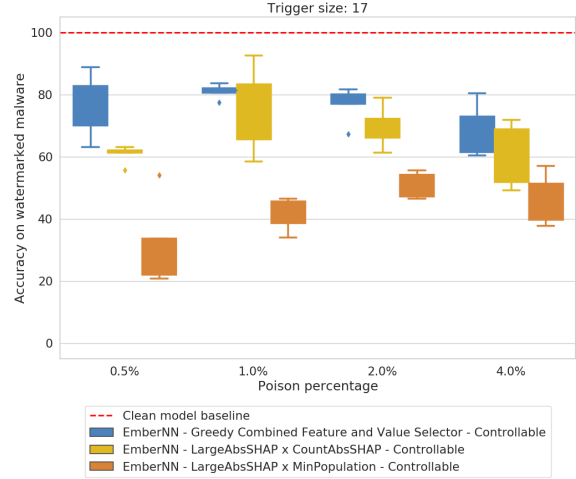
Lastly, we evaluate the scenario in which the attacker has access to only a small subset of clean training data and uses the same model architecture as the victim (i.e., *data_limited*). We perform this experiment by training a LightGBM model with 20% of the training data and using it to generate the trigger, which we then used to attack the LightGBM model trained over the entire dataset. Using the *Independent* strategy with *LargeAbsSHAP* and *CountAbsSHAP* over 16 features and a 1% poison set size, we noticed very little difference compared to the same attack where the SHAP values are computed over the entire training set ($\approx 4\% \Delta Acc(F_b, X_b)$).

6 Problem-Space Considerations

In the previous section, we explored model-agnostic attack strategies when the attacker has full control of the features

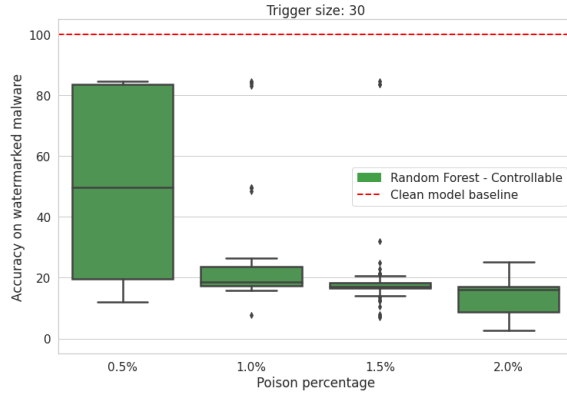


(a) LightGBM target

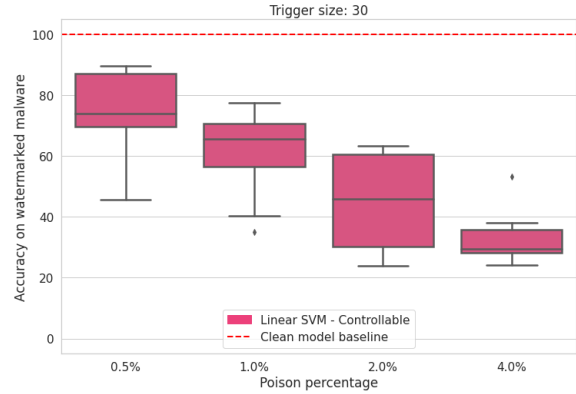


(b) EmberNN target

Figure 4: Accuracy of the backdoor model over watermarked malicious samples. Lower $Acc(F_b, X_b)$ is the result of stronger attacks. The watermark uses the subset of 17 features of EMBER, modifiable by the *constrained* adversary.



(a) Random Forest classifier on Contagio data.



(b) Linear SVM classifier on Drebin data.

Figure 5: 50 attack runs for Contagio and 10 for Drebin, using the *Combined* strategy, with a 30-features trigger.

and can change their values at will. A *constrained* attacker has to expend non-trivial effort to ensure that the backdoor generated in *feature-space* does not break the semantics or otherwise compromise the functionality of binaries in the *problem-space* [47]; that is backdoored goodwill must maintain the original label and watermarked malware retain its malicious functionality.

6.1 Windows PEs

We implemented a backdooring utility using the *pefile* [19] library to create a generic tool that attempts to apply a given watermark to arbitrary Windows binaries. Creating this utility in a sufficiently general way required specialized knowledge of the file structure for Windows Portable Executable (PE) files, in particular when adding sections to the binaries. Doing so required extending the section table with the appropriate sections, names, and characteristics, which in turn meant re-locating structures that follow the section table, such as data

directories and the sections themselves, to allow for arbitrary increases in the number of sections added.

We also encountered several challenges that required us to drop certain features and consider dependencies among features that restrict the values they can take on. First, we realized that the vast majority of the features in EMBER are based on feature hashing, which is often used to vectorize arbitrarily large spaces into a fixed-length vector. For example, strings uncovered in the binary may be hashed into a small number of buckets to create a fixed-number of counts. Given the preimage resistance of the hash function, directly manipulating these features by tampering with the binary would be extremely difficult, and consequently we discard all hash-based features, leaving us with just 35 directly-editable, non-hashed features. Next, we considered dependencies among the non-hashed features. As it turns out, many of the features are derived from the same underlying structures and properties of the binary, and may result in conflicting water-

marks that cannot be simultaneously realized. For example, the *num_sections* and *num_write_sections* features are related because each time we add a writeable section, we necessarily increase the total number of sections. To handle these dependencies, we remove any features whose value is impacted by more than one other feature (e.g., *num_sections*). This allows us to keep the maximal number of features without solving complex constraint optimization problems. The last challenge arose from the question of how to handle natural constraints of the problem space, such as cases where the watermark might require us to remove URLs or reduce the file size. Here, the attacker has two choices: reduce the set of files that can be successfully watermarked or reduce the effectiveness of the watermark by adding constraints to the search algorithm that ensure maximal applicability, as shown in Section 4. Due to the large number of available Windows PE samples, we decided it was best for the attacker to sacrifice the samples, rather than lose attack effectiveness. Later, we will show the opposite case for Android malware, where imposing constraints on the watermark was the preferable solution.

After reducing our set of features based on the above criteria, we are left with 17 features that our generic watermarking utility can successfully manipulate on arbitrary Windows binaries. Examples of backdoor patterns can be found in Table 4, Appendix A.2. As we will see, despite the significant reduction in the space of available features, our proposed attack strategies still show significant effectiveness. While developing the watermarking utility was challenging, we believe it is well within the capabilities of a determined attacker, and can subsequently be reused for a variety of attack campaigns.

Attack Efficacy. As shown in Figure 4, the effectiveness of the attack is slightly decreased when the backdoor trigger is generated using only the 17 manipulable features supported by our watermarking utility. Such a *constrained* adversary, is, as expected, strictly less powerful than the *unrestricted* attacker we explored in Section 5. On the other hand, despite the strong limitations introduced to ease practical implementation, we argue that the average accuracy loss is still extremely relevant given the security critical application. Moreover, if we allow the poison size to grow to 2% of the overall training set, we obtain $Acc(F_b, X_b)$ levels comparable with the *unrestricted* at 1% poison size on LightGBM.

To explore additional realistic scenarios, we combined the limitation over features control with lack of access to the original model, *constrained - transfer*. As in Section 5.2, we generated the watermark using a surrogate model, with the most effective *transfer* strategy we identified before, but this time restricted to the controllable features. We observed an average $Acc(F_b, X_b)$ of 54.53% and 56.76% for LightGBM and EmberNN respectively. An even weaker and stealthier attacker could be obtained combining the characteristics of the previous adversary with a limited knowledge of the training data and the use of the *Combined* strategy. We evaluate

the effect of this *constrained - transfer - data_limited* adversary, with a backdoor computed using an EmberNN surrogate, with access to only 20% of the training set and applied to a LightGBM victim. Despite the extreme limitations imposed on the attacker, the effect on the model is still significant, with decreases in accuracy on points containing the trigger ranging from $\approx 10.8\%$ at 1% poisoning, up to $\approx 40\%$ for a 4% poisoning rate.

Lastly, we looked at the *constrained - black_box* scenario, where we produced the SHAP values for only the manipulable features using the SHAP KernelExplainer, which operates purely by querying the model as a black-box. We target LightGBM, with the *LargeAbsSHAP x CountAbsSHAP* strategy, poisoning 1% of the training set. The resulting model exhibits an average $Acc(F_b, X_b)$ of 44.62%, which makes this attacker slightly weaker than one having access to model-specific SHAP explainers. It is relevant to note here, that the adversary has to spend a significant amount of computation time to use the SHAP KernelExplainer.

Behavior Preservation. We randomly selected the 100 goodware and 100 malware binaries from our dataset and poisoned each of them with the backdoor for the LightGBM and EmberNN models, resulting in a total of 200 watermarked binaries for each model. To determine the watermark effects on the binaries' functionality, we run each sample in a dynamic analysis sandbox, which uses a variety of static, dynamic, and behavioral analysis methods to determine whether a binary is malicious. This experiment helps evaluate three important aspects of our attack when applied in the real world: (i) the ability to keep the original labels on watermarked goodware, (ii) the ability to maintain the original malicious functionality of the watermarked malware, and (iii) the impact of semantic restrictions on the features the adversary can use to carry out the poisoning. The original and backdoored binaries were submitted to a dynamic analysis environment with an execution timeout of 120 seconds. Table 5, in Appendix A.2, shows the results of our experiments. In the case of the LightGBM and EmberNN watermarks, both goodware and malware have similar numbers of failed watermarking attempts due to the physical constraints on the binaries, with the most prevalent reason (>90%) being binaries that were too large for the selected *size* watermark. For those files that were successfully watermarked, we observed that goodware always maintained its original benign label, while malware retained its malicious functionality in 61-66% of the cases. We also scanned our watermarked binaries with ESET and Norton AntiVirus signature-based antivirus engines, similar to those used by crowdsourced threat intelligence feeds, and found that none of the goodware changed labels due to the presence of our backdoor. Overall, this indicates that an attacker could use up to 75% of the observed goodware and 47% of the observed malware in these threat intelligence feeds to launch their backdoor poisoning attack. This is sufficient in real-world attacks as the adversary needs a small percentage of poisoned binaries

to execute the attack. Finally, it is important to point out that our evaluation here focused on an adversary using commodity goodwill and malware. However, an advanced attacker may produce their own software to better align with the chosen watermark values and maximize the attack impact.

6.2 Other Datasets

PDF files and Android applications have been the object of a large body of research on malware classification and classifier evasion. Therefore, we focused on these two domains as examples for the adaptability of our explanation-based attack.

PDF Files. We worked with the Contagio³ PDF data, consisting of 10,000 samples evenly distributed between benign and malicious, with 135-dimensional feature vectors extracted according to PDFRate [57] specification. To ensure our modifications were behavior-preserving, we developed a Python 3 port of the feature editor released⁴ with Mimicus [58]. This tool allowed us to parse the PDF files, apply the desired backdoor pattern, and read back a new feature vector after the poisoning to account for possible side effects, such as alterations in various size-based features.

Unfortunately, during our experimentation we ran into several bugs in the Mimicus feature editor that lead to inconsistent application of our otherwise valid watermark to the PDFs. In particular, these issues forced us to reduce our trigger pattern to only 30 of the 35 features reported as modifiable in the paper, and to restrict our poisoning pool to only those files that were correctly backdoored. Fixing these issues is beyond the scope of this work, but despite these limitations we were still able to poison enough samples to mount successful attacks.

Android Applications. In the Android domain, we used the well-studied Drebin [12] dataset containing 5,560 malicious and 123,453 benign apps, represented by Boolean vectors indicating which of the over 545,000 statically extracted features are present in the application. Such a large space of features is divided into 8 logical subsets, $S_1 - S_4$ being characteristics of the Android *manifest* file, and $S_5 - S_8$ being extracted from the disassembled code.

To ensure no loss of functionality was inadvertently sustained as side effect of the trigger application, we borrowed the technique specified by Grosse et al. [26, 27]. First, we restricted ourselves to only altering features belonging to subsets S_1 and S_2 , representing the list of *hardware components* and the list of *permissions* requested by the application, respectively. Both these subsets belong to the manifest class of features and can be modified by changing a single line in the manifest file. Second, we forced our backdoor to be exclusively additive, meaning that no feature could be removed from an application as result of the poisoning.

³<http://contagiodump.blogspot.com/>

⁴<https://github.com/sndic/mimicus>

Other advanced (and computationally expensive) techniques may also be used to increase the number of manipulable features available to our attack strategy while still ensuring behavior preservation, such as *organ harvesting* [47] for adversarial Android malware or behavioral *oracles* [69] for PDF files. We believe that the improvement of feature-space to problem-space mapping methods, will greatly improve the effectiveness of explanation-guided poisoning attacks.

Attack Efficacy. Having observed how our *Combined* strategy is both stealthy (more on this in Section 7), and especially adept at generating behavior preserving backdoors, we employed it for our experiments on the Contagio and Drebin datasets. In both cases, we use the original model architecture proposed in the literature, therefore, we test our attack on a Random Forest classifier for the PDF files, and a Linear Support Vector Machine (SVM) classifier for the Android applications.

Figure 5a shows the reduction in accuracy of the poisoned Random Forest induced by our *constrained* adversary. It is interesting to observe that, probably due to the small size of the dataset combined with the necessity of limiting the poisoning pool to only the PDF files correctly modified by the editor utility, there appears to be a large amount of variance in the attack effectiveness at lower poison percentages. These effects fade away with larger poisoning pools. Overall, the attack is generally very successful, inducing, for instance, an average 21.09% $Acc(F_b, X_b)$, at 1.5% poisoning rate.

Applying the explanation attack to the Android data proved somewhat more challenging due to the sparsity of the feature space. To handle the dimensionality issue, we first used L1 regularized logistic regression to select a subset of 991 features, then we trained a surrogate LightGBM model and used the surrogate to compute the SHAP values. This corresponds to a *transfer-constrained* adversary. A 30-feature backdoor thus computed was then applied to the original 545K-dimensional vectors used to train the Linear SVM. Figure 5b shows the effect of the poisoning on the accuracy of the model on backdoored malware. For instance, at 2% poisoning rate, the attack lowers the model accuracy on backdoored samples to 42.9% on average. We also observed minimal loss of $Acc(F_b, X)$ within 0.03%, and change in FP_b , less than 0.08%, on average.

7 Mitigation

Recently, researchers started tackling the problem of defending against backdoor attacks [20, 37, 64, 67]. Nearly all existing defensive approaches, however, are specifically targeted at computer vision Deep Neural Networks, and assume adversaries that actively tamper with the training labels. These limitations make them hard to adapt to the class of model-agnostic, clean-label attacks we are interested in. We discuss here representative related work.

Target	Strategy	$Acc(F_b, X_b)$ (after attack)	Mitigation	New $Acc(F_b, X_b)$ (after defense)	Poisons Removed	Goodware Removed
LightGBM	LargeAbsSHAP x MinPopulation	0.5935	HDBSCAN	0.7422	3825	102251
			Spectral Signature	0.7119	962	45000
			Isolation Forest	0.9917	6000	11184
	LargeAbsSHAP x CountAbsSHAP	0.5580	HDBSCAN	0.7055	3372	93430
			Spectral Signature	0.6677	961	44999
			Isolation Forest	0.9921	6000	11480
	Combined Feature Value Selector	0.8320	HDBSCAN	0.8427	1607	115282
			Spectral Signature	0.7931	328	45000
			Isolation Forest	0.8368	204	8927
EmberNN	LargeAbsSHAP x MinPopulation	0.4099	HDBSCAN	0.3508	3075	137597
			Spectral Signature	0.6408	906	45000
			Isolation Forest	0.9999	6000	14512
	LargeAbsSHAP x CountAbsSHAP	0.8340	HDBSCAN	0.5854	2499	125460
			Spectral Signature	0.8631	906	45000
			Isolation Forest	0.9999	6000	15362
	Combined Feature Value Selector	0.8457	HDBSCAN	0.8950	1610	120401
			Spectral Signature	0.9689	904	45000
			Isolation Forest	0.8030	175	13289

Table 3: Mitigation results for both LightGBM and EmberNN. All attacks were targeted towards the 17 controllable features (see Section 6), with a 1% poison set size, 6000 backdoored benign samples. We show $Acc(F_b, X_b)$ for the backdoored model, and after the defense is applied. We also include number of poisoned and goodwill points filtered out by the defensive approaches.

Tran et al. [64] propose a defensive method based on *spectral signatures*, which relies on detecting two ϵ -spectrally separable subpopulations based on SVD decomposition. Chen et al. [20] rely on the representation learned by the CNN and perform k-means clustering on the activations of the last convolutional layer. The defense of Liu et al. [37] is based on combining network fine tuning and neuron pruning, making it specific to neural networks. Finally, NeuralCleanse [67] is based on the intuition that in a backdoored model, the perturbation necessary to induce a misclassification towards the targeted class should be smaller than that required to obtain different labels. This approach was designed considering multi-class classification problem, as encountered in image recognition, and the suggested filtering and pruning mitigation are neural-network specific.

Considered Defensive Approaches. According to our threat model, the defender is assumed to: (i) have access to the (poisoned) training data; (ii) have access to a small set of clean labeled data. This common assumption in adversarial ML fits nicely with the context since security companies often have access to internal, trusted, data sources; and (iii) know that the adversary will target the most relevant features.

We evaluate three mitigation strategies over a reduced feature space obtained by selecting a fixed number (32) of the most important features. First, a state-of-the-art defensive strategy, spectral signatures [64], which we adapt by computing the singular value decomposition of the benign samples over the new feature space. Then, as in the original paper, we compute the *outlier score* by multiplying the top right singular vector and we filter out the samples with the highest 15% scores. Second, hierarchical density-based clustering, (HDBSCAN) [16], inspired by Chen et al’s [20] use of k-means for defensive clustering over neuron activations. We

borrow the idea, using HDBSCAN instead, with the intuition that watermarked samples form a subspace of high density in the reduced feature space, and generate a tight cluster. Additionally, HDBSCAN does not require a fixed number of clusters, but has two other parameters that control the cluster density (minimum size of a cluster, set at 1% of the training benign data, 3000 points, and minimum number of samples to form a dense region, set at 0.5%, 600 points). As in [20], we compute Silhouette scores on the resulting clusters, to obtain an estimate of the intra-cluster similarity of a sample compared to points from its nearest neighboring cluster, and filter out samples from each cluster with a probability related to the cluster silhouette score. Third, isolation forest [36], an algorithm for unsupervised anomaly detection based on identifying rare and different points instead of building a model of a normal sample. The intuition here is that such an anomaly detection approach might identify the watermarked samples as outliers due to their similarity compared to the very diverse background points. We experiment with default parameters of Isolation Forest.

Results of Mitigation Strategies. Table 3 shows the effect of these three mitigation strategies over the different models and attack strategies. Two main takeaways emerge from these empirical results. First, the Isolation Forest, trained on the reduced feature space, is often capable of correctly isolating all the backdoored points with relatively low false positives. Note that this happens exclusively when an Isolation Forest is trained on the transformed dataset (reduced to most important features). The same algorithm applied in the original feature space detects only a tiny fraction of the backdoored points ($\approx 1\%$), with similar results obtained also on Drebin (0%) and Contagio (12.5%), thus reinforcing the observation in [64] that the subpopulations are not sufficiently separable

in the original feature space. Second, none of the mitigation approaches was able to isolate the points attacked with watermarks produced with the *Combined* strategy on PE files. This confirms that the *Combined* attack strategy is much more stealthy compared to both *Independent* strategies.

We note that the proposed mitigations are only a first practical step in defending against clean-label backdoor attacks in a model-agnostic setting. We leave a deeper investigations of more general defensive methods, as a topic of future work. Protecting ML systems from adversarial attacks is an intrinsically hard problem [18]. We argue that defending against our backdoor attacks is extremely challenging due to the combined effect of the small subpopulation separability induced by clean-label attacks, and the difficulty of distinguishing dense regions generated by the attack from other dense regions naturally occurring in diverse sets of benign binaries.

8 Related Work

An early line of research introduced by Perdisci et al. [46] and Newsome et al. [45] demonstrated methods for polluting automated polymorphic worm detectors such as Polygraph [44]. The first [46] introduced purposely crafted noise in the traces used for signature generation to prevent the generation of useful signatures; the second [45] proposed *red herring* attacks, where the goal of the adversary is to force the generated system to rely on spurious features for classification, which will then be excluded from the evading sample. Red herring attacks are particularly interesting for us, being the first to suggest that an adversary does not necessarily need control over data labels in order to cause failures in the downstream classifier, thus foreshadowing *clean-label* poisoning. Successive work by Venkataraman et al. [66] generalizes these results by providing lower bounds on the number of mistakes made by a signature generation algorithm based on conjunctions of boolean features. Theoretical bounds on poisoning attacks against an online centroid anomaly detection method have subsequently been analyzed by Kloft and Laskov [32] in the context of network intrusion detection. Concurrently, researchers started to analyze possible countermeasures to poisoning attempts against anomaly detection systems deployed to discover abnormal patterns in network traces. Cretu et al. [23] developed a methodology to sanitize training data based on the output of an ensemble of micro models, trained on small portions of the data, combined through simple voting schemes. Rubinstein et al. [51] later proposed to leverage methods from robust statistics to minimize the effect of small poison quantities on network traffic anomaly detectors based on Principal Component Analysis.

More recent research by Biggio et al. [14] brought to light the problem of poisoning attacks against modern machine learning models by proposing an availability attack based on gradient ascent against support vector machines. Successive work [15], demonstrated the relevance of ML poisoning

in the domain of malware classification by targeting Malheur [50], a malware behavioral clustering tool. Later research by Xiao et al. [68] showed that feature selection methods, like LASSO, ridge regression, and elastic net, were susceptible to small poison sizes. Gradient-based poisoning availability attacks have been shown against regression [29] and neural networks [43], and the transferability of these attacks has been demonstrated [24]. Recently, Suciú et al. [60] proposed a framework for defining attacker models in the poisoning space, and developed StingRay, a multi-model target poisoning attack methodology.

Backdoor attacks were introduced by Gu et al. in BadNets [28], identifying a supply chain vulnerability in modern machine learning as-a-service pipelines. Liu et al. [38] explored introducing trojan triggers in image recognition Neural Networks, without requiring access to the original training data, by partially re-training the models. Later works by Turner et al. [65] and Shafahi et al. [55] further improved over the existing attacks by devising clean-label strategies.

9 Discussion and Conclusion

With this work we begin shedding light on new ways of implementing clean-label backdoor attacks, a threat vector that we believe will only grow in relevance in the coming years. We showed how to conduct backdoor poisoning attacks that are model-agnostic, do not assume control over the labeling process, and can be adapted to very restrictive adversarial models. For instance, an attacker with the sole knowledge of the feature space can mount a realistic attack by injecting a relatively small pool of poisoned samples (1% of training set) and induce high misclassification rates in backdoored malware samples. Additionally, we designed the *Combined* strategy that creates backdoored points in high-density regions of the legitimate samples, making it very difficult to detect with common defenses. Based on our exploration of these attacks, we believe explanation-guided attack strategies could also be applicable to other feature-based models, outside of the security domain.

Finally, there are some limitations of this work that we would like to expose. First, the attacks we explored rely on the attacker knowing the feature space used by the victim model. While this assumption is partially justified by the presence of natural features in the structure of executable files, we consider the development of more generic attack methodologies, which do not rely on any knowledge from the adversary’s side, as an interesting future research direction. Second, designing a general mitigation method, particularly against our stealthy *Combined* attack strategy, remains a challenging problem for future work. Lastly, adaptation of these attacks to other malware classification problems that might rely on combining static and dynamic analysis is also a topic of future investigation.

Acknowledgments

We would like to thank Jeff Johns for his detailed feedback on a draft of this paper and many discussions on backdoor poisoning attacks, and the anonymous reviewers for their insightful comments and valuable suggestions. We thank FireEye for sponsoring research done at Northeastern University for this project. The work done at Northeastern University was also partially sponsored by the U.S. Army Combat Capabilities Development Command Army Research Laboratory and was accomplished under Cooperative Agreement Number W911NF-13-2-0045 (ARL Cyber Security CRA). The views and conclusions contained in this document are those of the authors and should not be interpreted as representing the official policies, either expressed or implied, of the Combat Capabilities Development Command Army Research Laboratory or the U.S. Government. The U.S. Government is authorized to reproduce and distribute reprints for Government purposes notwithstanding any copyright notation

References

- [1] AlienVault - Open Threat Exchange. <https://otx.alienvault.com/>.
- [2] CylancePROTECT Malware Execution Control. https://www.cylance.com/content/dam/cylance/pdfs/feature-focus/Feature_Focus_PROTECT_Malware_Control.pdf.
- [3] Detonating a bad rabbit: Windows Defender Antivirus and layered machine learning defenses. <https://www.microsoft.com/security/blog/2017/12/11/detonating-a-bad-rabbit-windows-defender-antivirus-and-layered-machine-learning-defenses/>.
- [4] Machine Learning Static Evasion Competition. <https://www.elastic.co/blog/machine-learning-static-evasion-competition>.
- [5] MalwareGuard: FireEye's Machine Learning Model to Detect and Prevent Malware. <https://www.fireeye.com/blog/products-and-services/2018/07/malwareguard-fireeye-machine-learning-model-to-detect-and-prevent-malware.html>.
- [6] MetaDefender Cloud | Homepage. <https://metadefender.opswat.com>.
- [7] Skylight Cyber | Cylance, I Kill You! <https://skylightcyber.com/2019/07/18/cylance-i-kill-you/>.
- [8] VirSCAN.org - Free Multi-Engine Online Virus Scanner. <https://www.virscan.org/>.
- [9] VirusTotal. <http://www.virustotal.com/>.
- [10] Brandon Amos, Hamilton Turner, and Jules White. Applying machine learning classifiers to dynamic Android malware detection at scale. In *2013 9th International Wireless Communications and Mobile Computing Conference (IWCMC)*, July 2013. ISSN: 2376-6506.
- [11] Hyrum S. Anderson and Phil Roth. EMBER: An Open Dataset for Training Static PE Malware Machine Learning Models. *arXiv:1804.04637 [cs]*, April 2018.
- [12] Daniel Arp, Michael Spreitzenbarth, Malte Hübner, Hugo Gascon, and Konrad Rieck. Drebin: Effective and Explainable Detection of Android Malware in Your Pocket. In *Proceedings 2014 Network and Distributed System Security Symposium*, San Diego, CA, 2014. Internet Society.
- [13] Battista Biggio, Iginio Corona, Davide Maiorca, Blaine Nelson, Nedim Šrndić, Pavel Laskov, Giorgio Giacinto, and Fabio Roli. Evasion Attacks against Machine Learning at Test Time. *Advanced Information Systems Engineering*, 7908, 2013.
- [14] Battista Biggio, Blaine Nelson, and Pavel Laskov. Poisoning attacks against support vector machines. In *Proceedings of the 29th International Conference on International Conference on Machine Learning*, ICML'12, Edinburgh, Scotland, June 2012. Omnipress.
- [15] Battista Biggio, Konrad Rieck, Davide Ariu, Christian Wressnegger, Iginio Corona, Giorgio Giacinto, and Fabio Roli. Poisoning behavioral malware clustering. In *Proceedings of the 2014 Workshop on Artificial Intelligent and Security Workshop - AISec '14*, Scottsdale, Arizona, USA, 2014. ACM Press.
- [16] Ricardo J. G. B. Campello, Davoud Moulavi, and Joerg Sander. Density-Based Clustering Based on Hierarchical Density Estimates. In *Advances in Knowledge Discovery and Data Mining*, volume 7819. Springer Berlin Heidelberg, Berlin, Heidelberg, 2013.
- [17] Nicholas Carlini. Adversarial machine learning reading list. <https://nicholas.carlini.com/writing/2018/adversarial-machine-learning-reading-list.html>, 2020.
- [18] Nicholas Carlini, Anish Athalye, Nicolas Papernot, Wieland Brendel, Jonas Rauber, Dimitris Tsipras, Ian Goodfellow, Aleksander Madry, and Alexey Kurakin. On Evaluating Adversarial Robustness. *arXiv:1902.06705 [cs, stat]*, February 2019.
- [19] Ero Carrera. erocarrera/pefile. <https://github.com/erocarrera/pefile>.
- [20] Bryant Chen, Wilka Carvalho, Nathalie Baracaldo, Heiko Ludwig, Benjamin Edwards, Taesung Lee, Ian Molloy, and Biplav Srivastava. Detecting Backdoor Attacks on Deep Neural Networks by Activation Clustering. *arXiv:1811.03728 [cs, stat]*, November 2018.
- [21] Xinyun Chen, Chang Liu, Bo Li, Kimberly Lu, and

- Dawn Song. Targeted Backdoor Attacks on Deep Learning Systems Using Data Poisoning. *arXiv:1712.05526 [cs]*, December 2017.
- [22] Zheng Leong Chua, Shiqi Shen, Prateek Saxena, and Zhenkai Liang. Neural Nets Can Learn Function Type Signatures From Binaries. In *USENIX Security Symposium*, 2017.
- [23] Gabriela F. Cretu, Angelos Stavrou, Michael E. Locasto, Salvatore J. Stolfo, and Angelos D. Keromytis. Casting out Demons: Sanitizing Training Data for Anomaly Sensors. In *2008 IEEE Symposium on Security and Privacy (sp 2008)*, Oakland, CA, USA, May 2008. IEEE. ISSN: 1081-6011.
- [24] Ambra Demontis, Marco Melis, Maura Pintor, Matthew Jagielski, Battista Biggio, Alina Oprea, Cristina Nita-Rotaru, and Fabio Roli. Why do adversarial attacks transfer? explaining transferability of evasion and poisoning attacks. In *28th USENIX Security Symposium (USENIX Security 19)*, pages 321–338, Santa Clara, CA, August 2019. USENIX Association.
- [25] Ian J. Goodfellow, Jonathon Shlens, and Christian Szegedy. Explaining and Harnessing Adversarial Examples. *arXiv:1412.6572 [cs, stat]*, December 2014.
- [26] Kathrin Grosse, Nicolas Papernot, Praveen Manoharan, Michael Backes, and Patrick McDaniel. Adversarial Perturbations Against Deep Neural Networks for Malware Classification. *arXiv:1606.04435 [cs]*, June 2016.
- [27] Kathrin Grosse, Nicolas Papernot, Praveen Manoharan, Michael Backes, and Patrick McDaniel. Adversarial Examples for Malware Detection. In *Computer Security – ESORICS 2017*, volume 10493. Springer International Publishing, Cham, 2017.
- [28] Tianyu Gu, Brendan Dolan-Gavitt, and Siddharth Garg. BadNets: Identifying Vulnerabilities in the Machine Learning Model Supply Chain. *arXiv:1708.06733 [cs]*, August 2017.
- [29] Matthew Jagielski, Alina Oprea, Battista Biggio, Chang Liu, Cristina Nita-Rotaru, and Bo Li. Manipulating machine learning: Poisoning attacks and countermeasures for regression learning. In *IEEE Symposium on Security and Privacy*, SP '18. IEEE CS, 2018.
- [30] Alex Kantchelian, Michael Carl Tschantz, Sadia Afroz, Brad Miller, Vaishaal Shankar, Rekha Bachwani, Anthony D Joseph, and J Doug Tygar. Better malware ground truth: Techniques for weighting anti-virus vendor labels. In *Proceedings of the 8th ACM Workshop on Artificial Intelligence and Security*, pages 45–56, 2015.
- [31] Dhilung Kirat and Giovanni Vigna. MalGene: Automatic Extraction of Malware Analysis Evasion Signature. In *Proceedings of the 22nd ACM SIGSAC Conference on Computer and Communications Security - CCS '15*, Denver, Colorado, USA, 2015. ACM Press.
- [32] Marius Kloft and Pavel Laskov. Online anomaly detection under adversarial impact. volume 9 of *Proceedings of Machine Learning Research*, pages 405–412, Chia Laguna Resort, Sardinia, Italy, 13–15 May 2010. JMLR Workshop and Conference Proceedings.
- [33] Bojan Kolosnjaji, Ambra Demontis, Battista Biggio, Davide Maiorca, Giorgio Giacinto, Claudia Eckert, and Fabio Roli. Adversarial Malware Binaries: Evading Deep Learning for Malware Detection in Executables. In *2018 26th European Signal Processing Conference (EUSIPCO)*, September 2018.
- [34] Marek Krčál, Ondřej Švec, Martin Bálek, and Otakar Jašek. Deep Convolutional Malware Classifiers Can Learn from Raw Executables and Labels Only. *ICLR 2018*, February 2018.
- [35] Ram Shankar Siva Kumar, Magnus Nyström, John Lambert, Andrew Marshall, Mario Goertzel, Andi Comissoner, Matt Swann, and Sharon Xia. Adversarial machine learning—industry perspectives. *3rd Deep Learning and Security Workshop (DLS)*, 2020.
- [36] Fei Tony Liu, Kai Ming Ting, and Zhi-Hua Zhou. Isolation Forest. In *2008 Eighth IEEE International Conference on Data Mining*, December 2008.
- [37] Kang Liu, Brendan Dolan-Gavitt, and Siddharth Garg. Fine-Pruning: Defending Against Backdooring Attacks on Deep Neural Networks. *arXiv:1805.12185 [cs]*, May 2018.
- [38] Yingqi Liu, Shiqing Ma, Yousra Aafer, Wen-Chuan Lee, Juan Zhai, Weihang Wang, and Xiangyu Zhang. Trojaning Attack on Neural Networks. In *Proceedings 2018 Network and Distributed System Security Symposium*, San Diego, CA, 2018. Internet Society.
- [39] Scott M. Lundberg, Gabriel Erion, Hugh Chen, Alex DeGrave, Jordan M. Prutkin, Bala Nair, Ronit Katz, Jonathan Himmelfarb, Nisha Bansal, and Su-In Lee. From local explanations to global understanding with explainable AI for trees. *Nature Machine Intelligence*, 2(1), January 2020.
- [40] Scott M Lundberg and Su-In Lee. A Unified Approach to Interpreting Model Predictions. In I. Guyon, U. V. Luxburg, S. Bengio, H. Wallach, R. Fergus, S. Vishwanathan, and R. Garnett, editors, *Advances in Neural Information Processing Systems 30*. Curran Associates, Inc., 2017.
- [41] Thomas Mandl, Ulrich Bayer, and Florian Nentwich. ANUBIS ANalyzing Unknown BINarieS The automatic Way. In *Virus bulletin conference*, volume 1, page 02, 2009.
- [42] Enrico Mariconti, Lucky Onwuzurike, Panagiotis Andriotis, Emiliano De Cristofaro, Gordon Ross, and Gianluca Stringhini. MaMaDroid: Detecting Android Malware by Building Markov Chains of Behavioral Models. In *Pro-*

- ceedings 2017 Network and Distributed System Security Symposium*, San Diego, CA, 2017. Internet Society.
- [43] Luis Muñoz-González, Battista Biggio, Ambra Demontis, Andrea Paudice, Vasin Wonggrassamee, Emil C. Lupu, and Fabio Roli. Towards Poisoning of Deep Learning Algorithms with Back-gradient Optimization. *arXiv:1708.08689 [cs]*, August 2017.
- [44] J. Newsome, B. Karp, and D. Song. Polygraph: automatically generating signatures for polymorphic worms. In *2005 IEEE Symposium on Security and Privacy (S P'05)*, May 2005. ISSN: 2375-1207.
- [45] James Newsome, Brad Karp, and Dawn Song. Paragraph: Thwarting Signature Learning by Training Maliciously. In *Recent Advances in Intrusion Detection*, volume 4219. Springer Berlin Heidelberg, Berlin, Heidelberg, 2006. Series Title: Lecture Notes in Computer Science.
- [46] R. Perdisci, D. Dagon, Wenke Lee, P. Fogla, and M. Sharif. Misleading worm signature generators using deliberate noise injection. In *2006 IEEE Symposium on Security and Privacy (S&P'06)*, Berkeley/Oakland, CA, 2006. IEEE.
- [47] Fabio Pierazzi, Feargus Pendlebury, Jacopo Cortellazzi, and Lorenzo Cavallaro. Intriguing Properties of Adversarial ML Attacks in the Problem Space. In *2020 IEEE Symposium on Security and Privacy (SP)*, San Francisco, CA, USA, May 2020. IEEE.
- [48] Edward Raff, Jon Barker, Jared Sylvester, Robert Brandon, Bryan Catanzaro, and Charles Nicholas. Malware Detection by Eating a Whole EXE. *arXiv:1710.09435 [cs, stat]*, October 2017.
- [49] Marco Tulio Ribeiro, Sameer Singh, and Carlos Guestrin. "Why Should I Trust You?": Explaining the Predictions of Any Classifier. In *Proceedings of the 22nd ACM SIGKDD International Conference on Knowledge Discovery and Data Mining - KDD '16*, San Francisco, California, USA, 2016. ACM Press.
- [50] Konrad Rieck, Philipp Trinius, Carsten Willems, and Thorsten Holz. Automatic analysis of malware behavior using machine learning. *Journal of Computer Security*, 19(4), 2011.
- [51] Benjamin I.P. Rubinstein, Blaine Nelson, Ling Huang, Anthony D. Joseph, Shing-hon Lau, Satish Rao, Nina Taft, and J. D. Tygar. ANTIDOTE: understanding and defending against poisoning of anomaly detectors. In *Proceedings of the 9th ACM SIGCOMM conference on Internet measurement conference - IMC '09*, Chicago, Illinois, USA, 2009. ACM Press.
- [52] Igor Santos, Felix Brezo, Xabier Ugarte-Pedrero, and Pablo G. Bringas. Opcode sequences as representation of executables for data-mining-based unknown malware detection. *Information Sciences*, 231, May 2013.
- [53] Joshua Saxe and Konstantin Berlin. Deep neural network based malware detection using two dimensional binary program features. In *2015 10th International Conference on Malicious and Unwanted Software (MALWARE)*, October 2015. ISSN: null.
- [54] Giorgio Severi, Tim Leek, and Brendan Dolan-Gavitt. Malrec: Compact full-trace malware recording for retrospective deep analysis. In *Detection of Intrusions and Malware, and Vulnerability Assessment*, volume 10885, Cham, 2018. Springer International Publishing.
- [55] Ali Shafahi, W. Ronny Huang, Mahyar Najibi, Octavian Suci, Christoph Studer, Tudor Dumitras, and Tom Goldstein. Poison Frogs! Targeted Clean-Label Poisoning Attacks on Neural Networks. In *Advances in Neural Information Processing Systems*, April 2018.
- [56] Andrii Shalaginov, Sergii Banin, Ali Dehghantanha, and Katrin Franke. Machine Learning Aided Static Malware Analysis: A Survey and Tutorial. In Ali Dehghantanha, Mauro Conti, and Tooska Dargahi, editors, *Cyber Threat Intelligence*, volume 70. Springer International Publishing, Cham, 2018.
- [57] Charles Smutz and Angelos Stavrou. Malicious PDF detection using metadata and structural features. In *Proceedings of the 28th Annual Computer Security Applications Conference on - ACSAC '12*, Orlando, Florida, 2012. ACM Press.
- [58] Nedim Srdic and Pavel Laskov. Practical Evasion of a Learning-Based Classifier: A Case Study. In *2014 IEEE Symposium on Security and Privacy*, San Jose, CA, May 2014. IEEE.
- [59] Octavian Suci, Scott E. Coull, and Jeffrey Johns. Exploring Adversarial Examples in Malware Detection. In *2019 IEEE Security and Privacy Workshops (SPW)*, San Francisco, CA, USA, May 2019. IEEE.
- [60] Octavian Suci, Radu Ma, Tudor Dumitras, and Hal Daume Iii. When Does Machine Learning FAIL? Generalized Transferability for Evasion and Poisoning Attacks. 2018.
- [61] Mukund Sundararajan, Ankur Taly, and Qiqi Yan. Axiomatic Attribution for Deep Networks. *arXiv:1703.01365 [cs]*, June 2017.
- [62] Christian Szegedy, Wojciech Zaremba, Ilya Sutskever, Joan Bruna, Dumitru Erhan, Ian Goodfellow, and Rob Fergus. Intriguing properties of neural networks. *arXiv:1312.6199 [cs]*, December 2013.
- [63] Kimberly Tam, Salahuddin J. Khan, Aristide Fattori, and Lorenzo Cavallaro. CopperDroid: Automatic Reconstruction of Android Malware Behaviors. Internet Society, 2015.
- [64] Brandon Tran, Jerry Li, and Aleksander Mądry. Spectral signatures in backdoor attacks. In *Proceedings of the 32nd International Conference on Neural Informa-*

tion Processing Systems, NIPS'18, Montréal, Canada, December 2018. Curran Associates Inc.

- [65] Alexander Turner, Dimitris Tsipras, and Aleksander Mađry. Clean-Label Backdoor Attacks. *Manuscript submitted for publication*, 2019.
- [66] Shobha Venkataraman, Avrim Blum, and Dawn Song. Limits of Learning-based Signature Generation with Adversaries. In *16th Annual Network & Distributed System Security Symposium Proceedings*, 2008.
- [67] Bolun Wang, Yuanshun Yao, Shawn Shan, Huiying Li, Bimal Viswanath, Haitao Zheng, and Ben Y. Zhao. Neural Cleanse: Identifying and Mitigating Backdoor Attacks in Neural Networks. In *2019 IEEE Symposium on Security and Privacy (SP)*, San Francisco, CA, USA, May 2019. IEEE.
- [68] Huang Xiao, Battista Biggio, Gavin Brown, Giorgio Fumera, Claudia Eckert, and Fabio Roli. Is Feature Selection Secure against Training Data Poisoning? In *International Conference on Machine Learning*, 2015.
- [69] Weilin Xu, Yanjun Qi, and David Evans. Automatically Evading Classifiers: A Case Study on PDF Malware Classifiers. In *Proceedings 2016 Network and Distributed System Security Symposium*, San Diego, CA, 2016. Internet Society.
- [70] Wei Yang, Deguang Kong, Tao Xie, and Carl A. Gunter. Malware Detection in Adversarial Settings: Exploiting Feature Evolutions and Confusions in Android Apps. In *Proceedings of the 33rd Annual Computer Security Applications Conference on - ACSAC 2017*, Orlando, FL, USA, 2017. ACM Press.

A Additional Results

Feature	LightGBM	EmberNN
major_image_version	1704	14
major_linker_version	15	13
major_operating_system_version	38078	8
minor_image_version	1506	12
minor_linker_version	15	6
minor_operating_system_version	5	4
minor_subsystem_version	5	20
MZ_count	626	384
num_read_and_execute_sections	20	66
num_unnamed_sections	11	6
num_write_sections	41	66
num_zero_size_sections	17	17
paths_count	229	18
registry_count	0	33
size	1202385	817664
timestamp	1315281300	1479206400
urls_count	279	141

Table 4: Watermarks for LightGBM and EmberNN used during feasibility testing.

Dataset	Label	Result	Count
Original	Goodware	Dynamic Benign Dynamic Malicious	100 0
	Malware	Dynamic Benign Dynamic Malicious	7 93
LightGBM	Goodware	Failed Dynamic Benign Dynamic Malicious	25 75 0
	Malware	Failed Dynamic Benign Dynamic Malicious	23 30 47
EmberNN	Goodware	Failed Dynamic Benign Dynamic Malicious	33 67 0
	Malware	Failed Dynamic Benign Dynamic Malicious	33 23 44

Table 5: Summary of results analyzing a random sample of 100 watermarked goodware and malware samples in the dynamic analysis environment.

Here the reader will find additional details on the experimental results and feature analysis that help providing a general idea on the effectiveness and feasibility of the studied attacks.

A.1 Attack Results

Table 6, Table 7, and Table 8 report additional experimental results for the multiple runs of the attack with different strategies. All the attacks were repeated for 5 times and the tables report average results.

A.2 Feasible Backdoor Trigger

With our watermarking utility we were able to control 17 features with relative ease. Table 4 shows the feature-value mappings for two example backdoor triggers computed on the LightGBM and EmberNN models, which we fed to the static and dynamic analyzers to gauge the level of label retention after the adversarial modification. Table 5 summarizes the results of the dynamic analyzer over 100 randomly sampled benign and malicious executables from the EMBER dataset.

Table 6: LargeAbsSHAP x CountAbsSHAP - All features. Average percentage over 5 runs.

Trigger Size	Poisoned Points	$Acc(F_b, X_b)$	$Acc(F_b, X)$	FP_b	Trigger Size	Poisoned Points	$Acc(F_b, X_b)$	$Acc(F_b, X)$	FP_b
4	1500	65.8713	98.6069	0.0114	16	3000	21.0122	99.0832	0.0073
4	3000	55.8789	98.5995	0.0116	16	6000	36.7591	99.0499	0.0082
4	6000	40.3358	98.6081	0.0116	16	12000	53.8470	99.0729	0.0079
4	12000	20.1088	98.6060	0.0118	32	3000	13.2336	99.0608	0.0078
8	1500	30.8596	98.6335	0.0114	32	6000	20.3952	99.1152	0.0070
8	3000	10.1038	98.6212	0.0115	32	12000	28.3413	99.0856	0.0074
8	6000	2.8231	98.6185	0.0116	64	3000	5.8046	99.0723	0.0084
8	12000	0.0439	98.5975	0.0121	64	6000	11.1986	99.0959	0.0078
16	1500	2.4942	98.6379	0.0114	64	12000	11.5547	99.0998	0.0070
16	3000	0.9899	98.6185	0.0114	128	3000	2.4067	99.0810	0.0075
16	6000	0.0205	98.5948	0.0116	128	6000	1.6841	99.0688	0.0075
16	12000	0.0138	98.6323	0.0117	128	12000	2.8298	99.1088	0.0074

LightGBM EmberNN

Table 7: LargeAbsSHAP x MinPopulation - All features. Average percentage over 5 runs.

Trigger Size	Poisoned Points	$Acc(F_b, X_b)$	$Acc(F_b, X)$	FP_b	Trigger Size	Poisoned Points	$Acc(F_b, X_b)$	$Acc(F_b, X)$	FP_b
4	1500	62.3211	98.5985	0.0115	16	3000	18.8691	99.1219	0.0074
4	3000	52.5933	98.6144	0.0114	16	6000	33.5211	99.0958	0.0079
4	6000	30.8696	98.6044	0.0116	16	12000	50.6499	99.0942	0.0080
4	12000	20.3445	98.5836	0.0118	32	3000	9.1183	99.1189	0.0075
8	1500	32.0446	98.6128	0.0114	32	6000	12.1103	99.0827	0.0078
8	3000	20.5850	98.6159	0.0115	32	12000	14.6766	99.1127	0.0071
8	6000	14.9360	98.6087	0.0115	64	3000	3.4980	99.1170	0.0075
8	12000	1.9214	98.6037	0.0117	64	6000	6.2418	99.1234	0.0072
16	1500	4.3328	98.6347	0.0114	64	12000	6.8627	99.0941	0.0075
16	3000	1.4490	98.6073	0.0115	128	3000	0.9514	99.0675	0.0082
16	6000	0.1670	98.6301	0.0115	128	6000	1.6012	99.0824	0.0082
16	12000	0.0026	98.6169	0.0118	128	12000	1.6200	99.0816	0.0074

LightGBM EmberNN

Table 8: Greedy Combined Feature and Value Selector - All features. Average percentage over 5 runs.

Trigger Size	Poisoned Points	$Acc(F_b, X_b)$	$Acc(F_b, X)$	FP_b	Trigger Size	Poisoned Points	$Acc(F_b, X_b)$	$Acc(F_b, X)$	FP_b
4	1500	63.3370	98.5976	0.0113	16	3000	11.6613	99.1014	0.0082
4	3000	60.6706	98.6320	0.0114	16	6000	11.0876	99.1105	0.0078
4	6000	54.3283	98.6211	0.0114	16	12000	10.5981	99.0958	0.0079
4	12000	40.2437	98.6099	0.0118	32	3000	4.8025	99.0747	0.0087
8	1500	49.5246	98.6290	0.0113	32	6000	5.0524	99.1167	0.0082
8	3000	37.3295	98.6153	0.0113	32	12000	4.4665	99.1335	0.0072
8	6000	23.6785	98.6147	0.0117	64	3000	1.9074	99.1012	0.0076
8	12000	17.7914	98.6282	0.0117	64	6000	1.8246	99.0989	0.0077
16	1500	0.8105	98.6195	0.0113	64	12000	1.8364	99.1117	0.0071
16	3000	0.6968	98.6170	0.0115	128	3000	0.7356	99.0926	0.0082
16	6000	0.0565	98.6241	0.0116	128	6000	0.7596	99.1219	0.0080
16	12000	0.0329	98.6173	0.0118	128	12000	0.7586	99.1014	0.0072

LightGBM EmberNN